




# The Arginine Biosynthesis Pathway of *Candida albicans* Regulates Its Cross-Kingdom Interaction with *Actinomyces viscosus* to Promote Root Caries

Kaixin Xiong,<sup>a</sup> Hualing Zhu,<sup>a</sup> Yanyao Li,<sup>a</sup> Mengzhen Ji,<sup>a</sup> Yujia Yan,<sup>a</sup> Xuan Chen,<sup>a</sup> Yaqi Chi,<sup>a</sup> Xueqin Yang,<sup>a</sup> Ling Deng,<sup>a</sup> Xuedong Zhou,<sup>a</sup> Ling Zou,<sup>b</sup>  Biao Ren<sup>a</sup>

<sup>a</sup>State Key Laboratory of Oral Diseases, National Clinical Research Center for Oral Diseases, West China School of Stomatology, Sichuan University, Chengdu, China

<sup>b</sup>State Key Laboratory of Oral Diseases, National Clinical Research Center for Oral Diseases, Department of Conservation Dentistry and Endodontics, West China School of Stomatology, Sichuan University, Chengdu, China

**ABSTRACT** The cross-kingdom interactions between *Candida albicans* and *Actinomyces viscosus* play critical roles in root caries. However, the key pathway by which *C. albicans* regulates its interactions with *A. viscosus* is unclear. Here, we first employed 39 volunteers with root caries and 37 caries-free volunteers, and found that the abundances of *C. albicans* and *A. viscosus* were significantly increased in the individuals with root caries and showed a strong positive correlation. Their dual-species combination synergistically promoted biofilm formation and root caries in rats. The arginine biosynthesis pathway of *C. albicans* was significantly upregulated in dual-species biofilms and dental plaques from another 10 root caries volunteers compared with the 10 caries-free volunteers. The exogenous addition of arginine increased the cariogenicity of the dual-species biofilm. The *C. albicans* *ARG4*, a key gene from the arginine biosynthesis pathway, null mutant failed to promote dual-species biofilm formation and root caries in rats; however, the addition of arginine restored its synergistic actions with *A. viscosus*. Our results identified the critical roles of the *C. albicans* arginine biosynthesis pathway in its cross-kingdom interactions with *A. viscosus* for the first time and indicated that targeting this pathway was a practical way to treat root caries caused by multiple species.

**IMPORTANCE** Root caries is a critical problem that threatens the oral health of the elderly population. Our results identified the essential roles of the *C. albicans* arginine biosynthesis pathway in its cross-kingdom interactions with *A. viscosus* in root caries for the first time and indicated that targeting this pathway was a practical way to treat root caries caused by multiple species.

**KEYWORDS** root caries, multispecies infection, *Candida albicans*, *Actinomyces viscosus*, arginine biosynthesis pathway

Oral diseases are a major health burden for many countries and affect individuals throughout their lifetimes, causing pain, discomfort, disfigurement, and even death (<https://www.who.int/news-room/fact-sheets/detail/oral-health>). Oral diseases affect approximately 3.5 billion people worldwide, of which 2.3 billion people suffer from permanent tooth caries, the most common oral problem (1). Root caries is among the important reasons for tooth loosening in the elderly population, with prevalence ranging from 25% to 100% (2–4). Facilitating the prevention and treatment of root caries is among the important missions necessary to achieve the plan “8020 better oral health for older people” proposed by the WHO (5).

Oral microorganisms have been indicated to play crucial roles in the development of root caries. *Actinomyces viscosus* is an early colonizing microorganism of the root surface and a key pathogenic agent for root caries. *A. viscosus* was found to be the

**Editor** Teresa R. O’Meara, University of Michigan

**Copyright** © 2022 Xiong et al. This is an open-access article distributed under the terms of the [Creative Commons Attribution 4.0 International license](https://creativecommons.org/licenses/by/4.0/).

Address correspondence to Ling Zou, [zouling@scu.edu.cn](mailto:zouling@scu.edu.cn), or Biao Ren, [renbiao@scu.edu.cn](mailto:renbiao@scu.edu.cn).

The authors declare no conflict of interest.

**Received** 1 March 2022

**Accepted** 6 June 2022

**Published** 13 July 2022

dominant bacterium in all plaque samples from root surface caries (6) and accounted for 100% of the isolation frequencies (7). The cariogenic factors of *A. viscosus* include the strong ability of cell adhesion (8) and the capability to metabolize several kinds of carbohydrates, such as starch, sucrose, glucose, and fructose, which results in the production of large amounts of acids and the rapid demineralization of the infected teeth (9). Acid production can also reduce the growth of other oral bacteria in root caries plaque because *A. viscosus* has a tolerance to acid (9).

*Candida albicans* is a common symbiotic fungus in the oral cavity, respiratory and digestive tracts, and urogenital system. *C. albicans* is highly associated with oral candidiasis (10) and dental caries in the oral cavity, especially in Early Childhood Caries (ECC) and root caries (11, 12). The isolation frequency of *C. albicans* in root caries lesions was found to be approximately 40% (13), while both the isolation frequency and detection abundance of *C. albicans* from root caries lesions were found to be much higher than those from sound root surfaces (12). *C. albicans* can penetrate into the dentin tubules and bind to collagen, and then secrete hydrolases to degrade collagen under acidic conditions to promote the caries process (14, 15).

The cross-kingdom interactions between *C. albicans* and many oral bacteria, such as *Streptococcus*, *Actinomyces*, *Fusobacterium*, and *Helicobacter* species, contribute to the development of different oral diseases (16–19). *C. albicans* and *Actinomyces* could coaggregate tightly, especially when *C. albicans* was in the hyphal state (20, 21). *C. albicans* and *streptococci* had a synergistic partnership, as *streptococci* promoted *C. albicans* to invade the oral mucosae, while *C. albicans* promoted *streptococci* to form biofilms on abiotic surfaces and in the oral cavity (18, 22, 23). Interactions between *Streptococcus mutans* and *C. albicans* could result in the formation of a more complicated biofilm with the elevation of extracellular polysaccharide production by *S. mutans* and hyphal formation of *C. albicans*, respectively, to promote dental caries development (16, 24–26). We also found that *C. albicans* could affect the interactions between *S. mutans* and *Streptococcus sanguinis* to promote the development of dental caries (12). *Streptococcus gordonii* could also promote *C. albicans* biofilm formation and hyphal development (17). *C. albicans* and *Staphylococcus aureus* synergistically interacted to promote pathogenic potential, increase resistance to antibiotics and help *Candida* circumvent the host immune system (27, 28). However, the key pathways by which *C. albicans* regulates its interactions with oral bacteria are still unclear.

We previously found that *C. albicans* increased the cariogenic abilities of *A. viscosus* *in vitro*, while voriconazole inhibited their cross-kingdom interactions (29, 30). However, the key pathway by which *C. albicans* regulates its cross-kingdom interactions with *A. viscosus* and the effects of their coinfection in root caries are still unclear. Thus, in this study, we aimed to identify the *C. albicans* pathway that is critical for its interactions with *A. viscosus* in clinical root caries samples, dual-species biofilms, and root caries rat models.

## RESULTS

**Increased detection rates and abundances of *C. albicans* and *A. viscosus* in root caries.** Seventy-six volunteers, including 39 patients with root caries in the root caries (RC) group and 37 healthy people in the healthy control (HC) group, were recruited to compare the detection rates and abundances of *C. albicans* and *A. viscosus* in supragingival dental plaque. The rate of *C. albicans* detection was 82.05% in the RC group and was significantly higher than that in the HC group (51.35%) (Fig. 1A;  $P < 0.05$ ). The rate of *A. viscosus* detection was 82.05% in the RC group and was also significantly higher than that in the HC group (70.27%) (Fig. 1B;  $P < 0.05$ ). The abundances of *C. albicans* and *A. viscosus* were also significantly enriched in the RC group ( $19.75 \pm 12.92$  copies/ng and  $41.84 \pm 23$  copies/ng, respectively) compared with those in the HC group ( $6.399 \pm 6.669$  copies/ng and  $18.57 \pm 11.33$  copies/ng, respectively) (Fig. 1C and D;  $P < 0.05$ ). Notably, the abundances of *C. albicans* and *A. viscosus* were positive (Fig. 1E), suggesting that there is a strong correlation between *C. albicans* and *A. viscosus* in root caries.

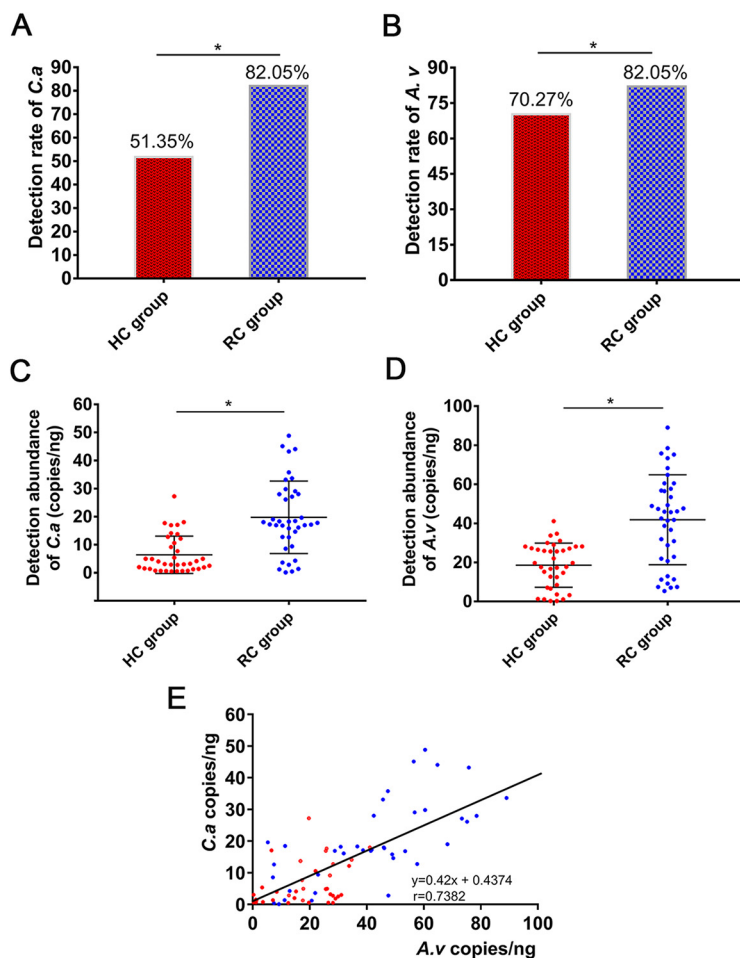


**FIG 1** Increased amounts of *C. albicans* and *A. viscosus* in root carious lesions. (A, B) Detection rates of *C. albicans* and *A. viscosus* by PCR in the RC and HC groups. (A) *C. albicans*; (B) *A. viscosus*. (\*,  $P < 0.05$ ). (C, D) The abundances of *C. albicans* and *A. viscosus* determined by qPCR in the RC and HC groups. (C) *C. albicans*; (D) *A. viscosus* (\*,  $P < 0.05$ ). (E) Correlation and linear regression analysis between the abundances of *C. albicans* and *A. viscosus* among the plaque samples of all recruited subjects. The red dots represented the samples from the HC group and the blue dots represented samples from the RC group. The Pearson correlation coefficient  $r$  value is 0.7382 ( $r = 0.7382$ ,  $r^2 = 0.5449$ ,  $P \leq 0.05$ ).

**Synergistic interactions between *C. albicans* and *A. viscosus* promoted biofilm formation and cariogenicity.** We then investigated the cariogenicity of the *C. albicans* and *A. viscosus* dual-species combinations due to their positive correlation in clinical samples. During biofilm formation, the adherence rate in the dual-species group (87.17%) was higher than that in the single-species groups (69.06% for *C. albicans*, 77.51% for *A. viscosus*) (Fig. 2A;  $P < 0.05$ ). The biofilm biomass and viable cells of the dual-species group were significantly elevated compared with those of the single-species groups (Fig. 2B and C;  $P < 0.05$ ). These results indicated that the combination of *C. albicans* and *A. viscosus* enhanced cell adherence, cell growth, and biofilm formation. The dual-species combination formed thicker and denser biofilms (Fig. 2D and E). A higher proportion of hyphal forms of *C. albicans* was observed in the dual-species biofilms than in the *C. albicans* mono-species biofilms (Fig. 2D and E). The numbers of both *C. albicans* and *A. viscosus* cells were elevated in the dual-species group (Fig. 2F and G). To test whether viable cell-cell contact is necessary for the enhanced biofilm formation, we combined viable cells, heat-killed cells, and cell supernatants of *C. albicans* and *A. viscosus*, respectively, and found that only the combination of viable cells significantly enhanced biofilm formation, indicating that cell-cell contact was essential for the interactions between *C. albicans* and *A. viscosus* (Fig. S1).

Moreover, the dual-species biofilm produced more water insoluble extracellular polysaccharides (EPS), the key cariogenic virulence factor, compared with that

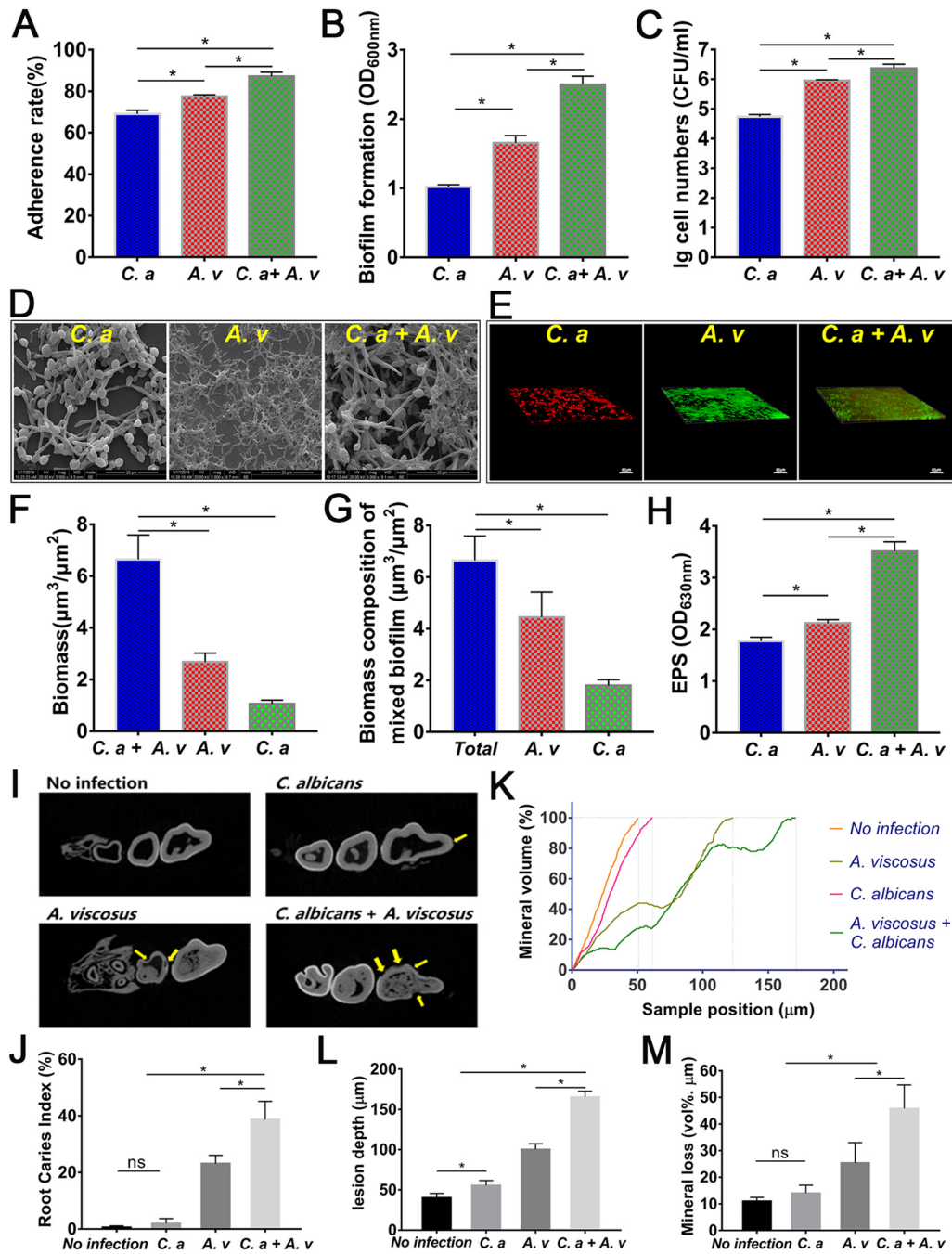


**FIG 2** *C. albicans* synergistically interacted with *A. viscosus* to promote the cariogenicity and root caries. (A to C) The adherence rates (A), biofilm formations (B), and CFU (C) from the three groups: *C. albicans* single-species; *A. viscosus* single species; *C. albicans* + *A. viscosus* dual-species (\*,  $P < 0.05$ ). (D, E) Structural observations of biofilms formed by *C. albicans*, *A. viscosus*, *C. albicans*, and *A. viscosus* through SEM (D) and FISH (E) analysis. *C. albicans* was stained with red color while *A. viscosus* was stained with green color. (F, G) Biomasses of the three kinds of biofilms from FISH observation result, quantitatively calculated by COMSTAT. (F) Biomasses of *C. albicans* single-species, *A. viscosus* single-species, and *C. albicans* + *A. viscosus* dual-species FISH-visualized biofilms, respectively, quantified by COMSTAT. (G) Biomass of *C. albicans* + *A. viscosus* FISH-visualized biofilm and the respective biomass compositions of *C. albicans* and *A. viscosus* in this dual-species biofilm (\*,  $P < 0.05$ ). (H) Water insoluble EPS productions of three groups: *C. albicans* single-species, *A. viscosus* single species, *C. albicans* + *A. viscosus* dual-species (\*,  $P < 0.05$ ). (I) Representative micro-CT images of rat jaws from uninfected rats and rats infected with *C. albicans*, *A. viscosus*, or *C. albicans* + *A. viscosus*, respectively. Yellow arrows indicated root carious lesions. (J) Root caries index scores according to Doff's system (\*,  $P < 0.05$ ; ns, not significant). (K) The mineral volume curves of teeth from uninfected rats and rats infected with *C. albicans*, *A. viscosus*, or *C. albicans* + *A. viscosus*, respectively. (L) The lesion depths curves of teeth from uninfected rats and rats infected with *C. albicans*, *A. viscosus*, or *C. albicans* + *A. viscosus*, respectively (\*,  $P < 0.05$ ). (M) The mineral losses of teeth from uninfected rats and rats infected with *C. albicans*, *A. viscosus*, or *C. albicans* + *A. viscosus*, respectively (\*,  $P < 0.05$ ; ns, not significant).

of *C. albicans* or *A. viscosus* single-species biofilms (Fig. 2H;  $P < 0.05$ ), indicating that the cross-kingdom interactions between *C. albicans* and *A. viscosus* enhanced cariogenicity.

**C. albicans synergized with A. viscosus to promote root caries in rats.** We further evaluated whether the cross-kingdom interactions of *C. albicans* and *A. viscosus* could promote the development of root caries in rat model. Rats infected with *C. albicans* alone formed very little root caries, while the rats infected with *A. viscosus* formed typical root caries, indicating the strong cariogenic ability of *A. viscosus* (Fig. 2I and J). Coinfection with *C. albicans* and *A. viscosus* synergistically increased the formation and severity of root caries compared to those of *C. albicans* or *A. viscosus* single-species infection (Fig. 2I and J). The rats coinfecting with *C. albicans* and *A. viscosus* had the highest root caries score, lowest mineral volume, and largest lesion depth and mineral loss of the jaw (Fig. 2J to M;  $P < 0.05$ ). These results demonstrated that *C. albicans* could synergize with *A. viscosus* to promote root caries *in vivo*.

**The highly activated C. albicans arginine biosynthesis pathway in dual-species biofilms.** To further identify the key pathway by which *C. albicans* regulates its synergistic interaction with *A. viscosus*, we analyzed the transcriptome of *C. albicans* from the dual-species biofilm compared with the *C. albicans* single-species biofilm (Fig. S2). There were 176 differentially expressed genes (DEGs) between the two groups ( $FDR < 5\%$ ,  $|\log_2\text{FoldChange}| > 1$ ). 96 genes were upregulated and 80 genes were downregulated in the dual-species biofilm (Fig. 3A; Fig. S2C). The expressions of genes related to arginine biosynthesis of *C. albicans* were significantly increased, while the expression of arginine degradation associated gene *CAR1* was significantly decreased (Fig. 3A). Kyoto Encyclopedia of Genes and Genomes (KEGG) analysis further confirmed that the DEGs were most enriched in the arginine biosynthesis pathway of *C. albicans* (Fig. 3B). Gene expressions in the arginine biosynthesis pathway, including that of *ARG1*, *ECM42*, *ARG3*, *ARG4*, *ARG5,6*, *ARG8*, and *CAR1*, were then confirmed by quantitative PCR (qPCR) analysis. The results confirmed that the expression levels of *ARG1*, *ECM42*, *ARG3*, *ARG4*, and *ARG5,6* were significantly upregulated and that the expression of *CAR1* was significantly downregulated in the dual-species biofilm compared with those in the *C. albicans* single-species biofilm (Fig. S3); this result was consistent with the transcriptome analysis (Fig. 3A), indicating the key roles of the arginine biosynthesis pathway in dual-species biofilm.

**Enhanced activation of the C. albicans arginine biosynthesis pathway in clinical root caries.** To further confirm that the arginine biosynthesis pathway of *C. albicans* was also upregulated in clinical root caries, another 20 volunteers, including 10 patients with root caries (RC group) and 10 caries-free individuals (HC group), were recruited. The expression levels of the genes associated with arginine biosynthesis (*ARG1*, *ARG3*, *ARG4*, and *ARG5,6*) were significantly elevated while *CAR1* expression was decreased in the root caries plaques in the RC group compared with those in the sound root surface plaques in the HC group (Fig. 3C), which was in line with the transcriptome analysis in the dual-species biofilms and indicated that the enrichment of the *C. albicans* arginine biosynthesis pathway played key roles in the development of root caries.

**The addition of arginine increased the growth and biofilm formation of C. albicans, A. viscosus, and their dual-species combination.** We further evaluated the effect of the corresponding product of the arginine biosynthesis pathway (arginine) on the growth of *C. albicans* and *A. viscosus*. As shown in Fig. 4, the addition of arginine promoted *C. albicans* biofilm formation, similar to the dual-species combination, compared with that in the group without arginine (Fig. 4A;  $P < 0.05$ ). More hyphal formation in the *C. albicans* single-species biofilm with the addition of arginine and the dual-species biofilm was observed (Fig. 4B). *C. albicans* formed denser and more compact biofilm with the addition of arginine (Fig. 4C), with higher biomass than that of *C. albicans* single-species biofilm without arginine (Fig. 4C and D;  $P < 0.05$ ). The addition of arginine also promoted the formation of *A. viscosus* biofilms. *A. viscosus* formed denser and more compact biofilms with a greater total biomass with the addition of arginine (Fig. 4E and F). Moreover, the addition of arginine also enhanced the formation of dual-species biofilm. The total biomass of the

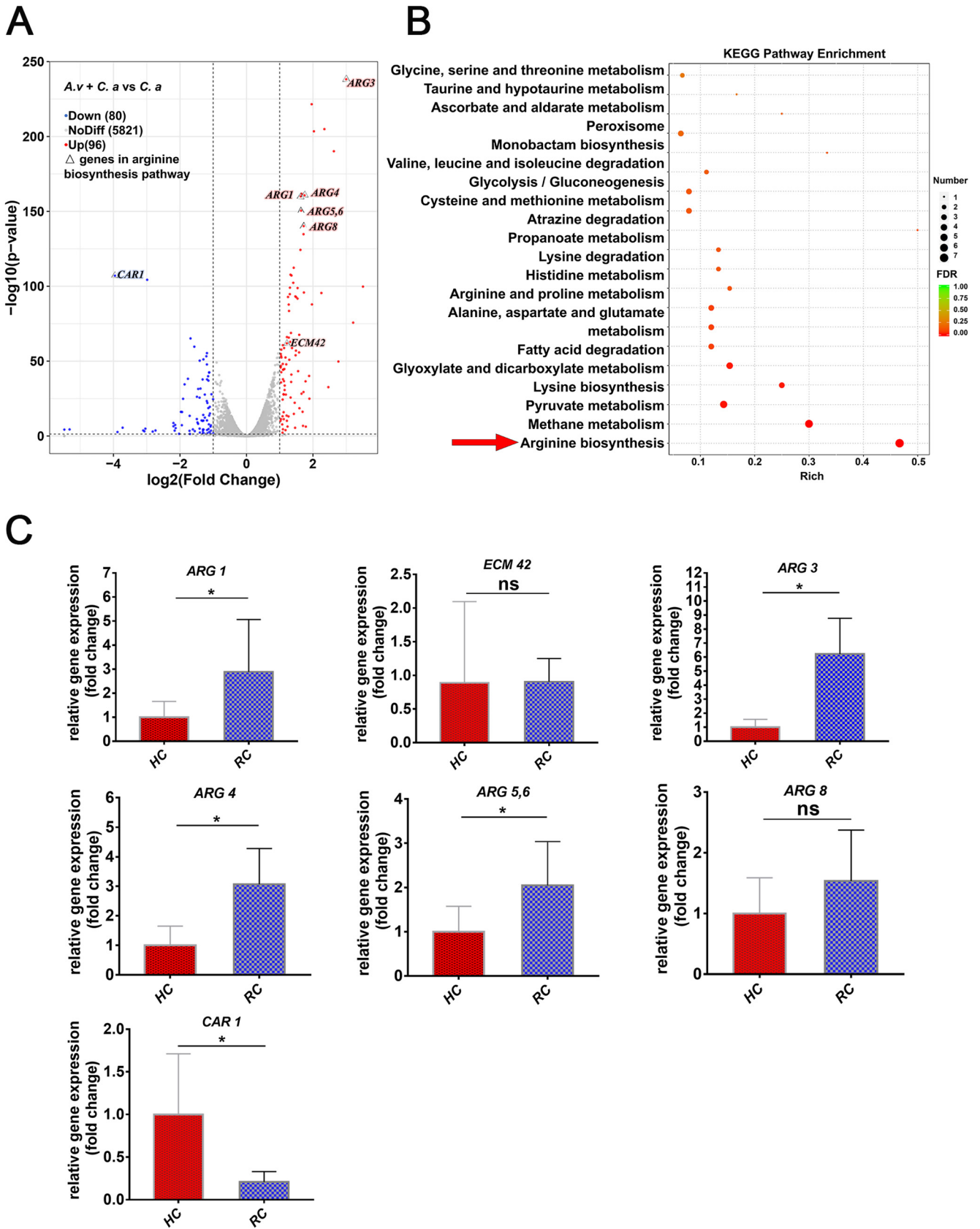


**FIG 3** Activation of the *C. albicans* arginine biosynthesis pathway in dual-species biofilm and clinical root caries plaque samples. (A) Volcano plot of centered and scaled FPKM values of DEGs indicating significant expression changes in the arginine biosynthesis pathway. The ARG1, ECM42, ARG3, ARG4, (Continued on next page)

dual-species biofilm with the addition of arginine was elevated significantly (Fig. 4G;  $P < 0.05$ ), suggesting that arginine increased the growth and biofilm formation of the *C. albicans* and *A. viscosus* combination.

**The *C. albicans* arginine biosynthesis pathway regulated its cross-kingdom interaction with *A. viscosus* in dual-species biofilms.** To confirm the essential role of the *C. albicans* arginine biosynthesis pathway in the regulation of its cross-kingdom interactions with *A. viscosus*, the *ARG4* null mutant (*arg4* $\Delta/\Delta$ ) was employed (Table S1). The *arg4* $\Delta/\Delta$  mutant failed to exhibit enhanced cell adhesion in both the dual-species and single-species groups compared with that of the wild-type (WT) strain, while the addition of arginine recovered the promotion (Fig. 5A). The *arg4* $\Delta/\Delta$  mutant exhibited reduced biofilm formation in both the dual-species and single-species biofilms compared to that of the WT strain, and the addition of arginine also reversed the reduction (Fig. 5B to D). In *C. albicans* WT and *A. viscosus* dual-species biofilm, the colonization of both *C. albicans* and *A. viscosus* were increased, compared with that in the single-species biofilm (Fig. 5D). However, the colonization of *C. albicans* in the *arg4* $\Delta/\Delta$  and *A. viscosus* dual-species biofilm was not obviously increased compared with that in the *arg4* $\Delta/\Delta$  single-biofilm (Fig. 5D). The addition of arginine restored the *C. albicans* colonization in the dual-species biofilm (Fig. 5D). These results indicated the essential roles of the arginine biosynthesis pathway of *C. albicans* in its cross-kingdom interactions with *A. viscosus* and suggested that targeting the arginine biosynthesis pathway could block their interaction in dual-species biofilm.

**The arginine biosynthesis pathway of *C. albicans* promoted root caries.** We then investigated the contribution of the arginine biosynthesis pathway of *C. albicans* to the development of root caries *in vivo*. In the rat root caries model, coinfection with *C. albicans* WT and *A. viscosus* caused the most remarkable root caries lesions (Fig. 6A, D;  $P < 0.05$ ), with elevated colonization of *C. albicans* and *A. viscosus* on the root surfaces (Fig. 6B, C;  $P < 0.05$ ). A reduced colonization of *arg4* $\Delta/\Delta$  was observed in the teeth (Fig. 6C;  $P < 0.05$ ). Combination of *arg4* $\Delta/\Delta$  and *A. viscosus* also failed to promote the colonization of *A. viscosus* (Fig. 6B;  $P < 0.05$ ) and the development of root caries (Fig. 6A, D;  $P < 0.05$ ), as the rats showed similar hard-tissue destruction, mineral volume, lesion depth and mineral loss compared to those of the rats infected by the *A. viscosus* single-species (Fig. 6D, G;  $P < 0.05$ ). However, the addition of arginine increased the colonization of *arg4* $\Delta/\Delta$  and *A. viscosus* in their combination (Fig. 6B, C;  $P < 0.05$ ). The addition of arginine enhanced the development of root caries in rats coinfecting with *arg4* $\Delta/\Delta$  and *A. viscosus* (Fig. 6A, D;  $P < 0.05$ ), and increased hard-tissue destruction, lesion depth and mineral loss and decreased mineral volumes (Fig. 6D, G;  $P < 0.05$ ), indicating that the *C. albicans* arginine biosynthesis pathway is essential for the development of root caries.

## DISCUSSION

The incidence of root caries has increased in recent years and it has become a major oral problem in the elderly population, but the treatment of root caries is challenging (2, 31). The prevention and treatment of root caries has become one of the major issues to improve oral health. *C. albicans* and *A. viscosus* are two resident symbiotic opportunistic microorganisms in the oral cavity (32, 33), and their cross-kingdom interactions play important roles in the development of root caries. We found that the isolation frequencies and abundances of both species were significantly higher in the root caries plaque samples than in the sound root surface plaque samples (Fig. 1A to D). The abundances of the two species showed a positive correlation (Fig. 1E).

The hyphal state of *C. albicans* is the main virulent form, and it can efficiently mediate microbial adhesion and biofilm formation process. In the dual-species biofilm, we found

### FIG 3 Legend (Continued)

*ARG5,6*, *ARG8*, and *CAR1* genes in the arginine biosynthesis pathway were marked. (B) KEGG pathway enrichment analysis indicating that the arginine biosynthesis pathway was the most DEG-enriched pathway. The yellow arrow showed the arginine biosynthesis pathway. (C) The differential expression of the arginine biosynthesis-associated genes: *ARG1*, *ECM42*, *ARG3*, *ARG4*, *ARG5,6*, *ARG8*, and the arginine degradation-associated gene: *CAR1* were confirmed from the root caries plaques (RC groups) compared with the HC groups by qPCR (\*,  $P < 0.05$ ; ns, not significant).

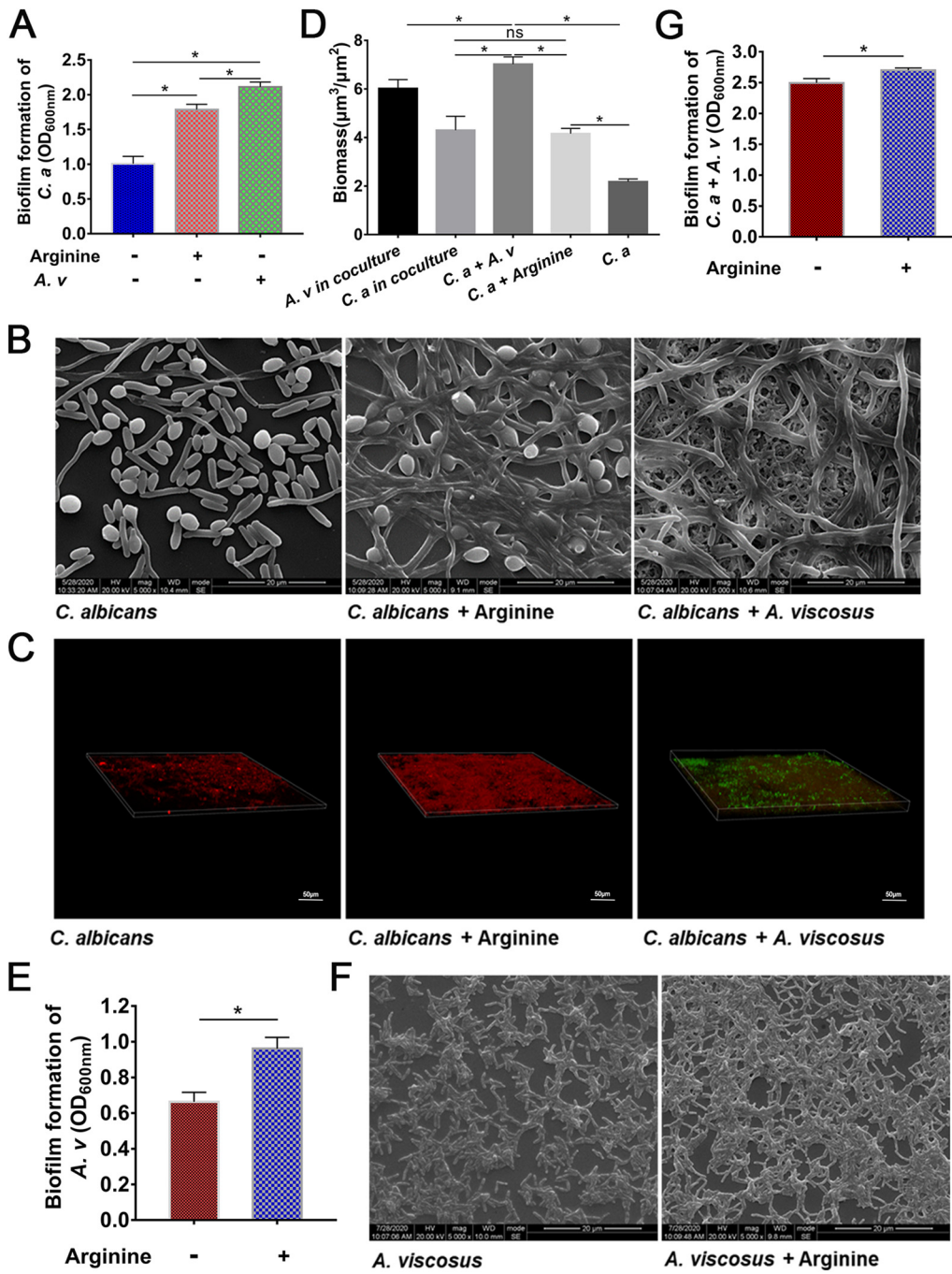


**FIG 4** The addition of arginine promoted the growth of *C. albicans*, *A. viscosus*, and dual-species biofilms. (A) Effect of arginine on *C. albicans* biofilm formation: Total biomasses quantified with CV assay of three kinds of biofilms formed by *C. albicans*, *A. viscosus*, *C. albicans* + *A. viscosus*, respectively (\*,  $P < 0.05$ ). (B, C) Effect of arginine on *A. viscosus* biofilm structure: Three structures of biofilms from *C. albicans*, *A. viscosus*, *C. albicans* + *A. viscosus*, respectively, observed with SEM and FISH. *C. albicans* was stained with red color while *A. viscosus* was stained with green color. (D) Biomasses of the biofilms according to FISH observation quantitatively calculated by COMSTAT (\*,  $P < 0.05$ ; ns, not significant). (E) Effect of arginine on the *A. viscosus* biofilm formation: Total biomasses of *A. viscosus* biofilm formed with or without arginine addition quantified by CV assay (\*,  $P < 0.05$ ). (F) Effect of arginine on *A. viscosus* biofilm structure: Structures of *A. viscosus* biofilm formed with or without arginine addition observed by SEM. (G) Effect of arginine on *A. viscosus* and *C. albicans* dual-species biofilm formation: Total biomasses of dual-species biofilm formed with or without arginine addition quantified by CV assay (\*,  $P < 0.05$ ).

that *A. viscosus* could promote the hyphal formation of *C. albicans*, thus promoting its virulence. Morse et al. (34) suggested that the coculture of *C. albicans* and *A. viscosus* could significantly increase the hyphal content in the biofilm, and the expression levels of *C. albicans* virulence genes, such as *ALS3*, *EPA1*, *PLD1*, *SAP4*, and *SAP6*, in the coculture biofilm were



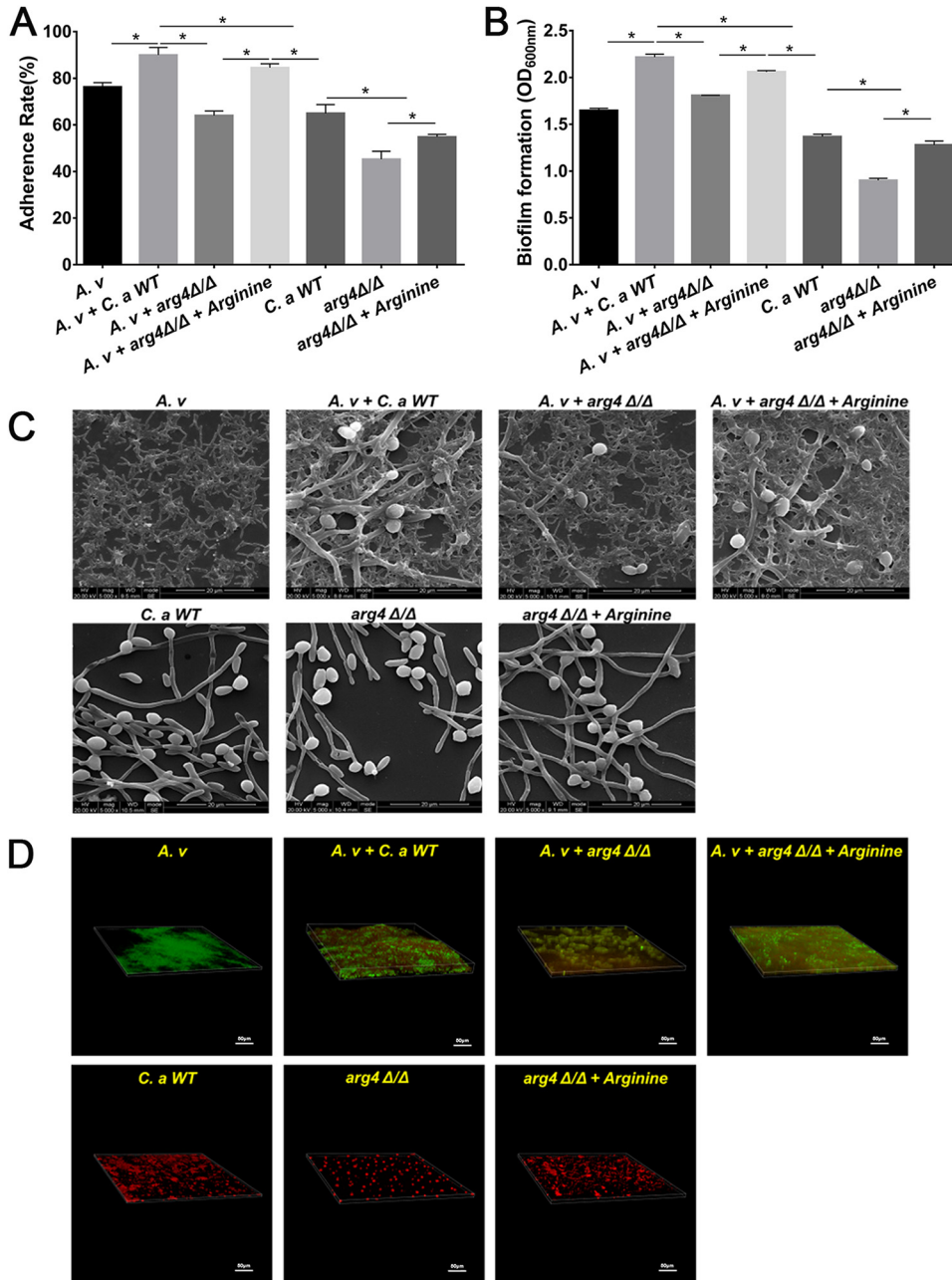


**FIG 5** *C. albicans* arginine biosynthesis pathway regulated cross-kingdom interactions in dual-species biofilms. (A, B) Determination of the effects of the *arg4Δ/Δ* mutant and arginine supplementation on *C. albicans* growth through adherence rate (A) and biofilm formation (B) (\*,  $P < 0.05$ ). (C, D) The biofilm structures of the *arg4Δ/Δ* mutant and with arginine supplementation determined via SEM (C) and FISH observations (D). *C. albicans* or *arg4Δ/Δ* mutant was stained with red color while *A. viscosus* was stained with green color.

significantly increased. Our previous work also showed that cariogenic virulence such as biofilm proliferation, acid production, acid resistance, sugar production, and biofilm formation were significantly enhanced under *C. albicans* and *A. viscosus* coculture conditions (30). However, the specific pathway by which *C. albicans* regulates the interactions between *C. albicans* and *A. viscosus* is still unclear. In our study, KEGG enrichment analysis of the RNA-Seq-identified DEGs suggested that the *C. albicans* arginine biosynthesis pathway, including six upregulated genes (*ARG1*, *ECM42*, *ARG3*, *ARG4*, *ARG5,6*, *ARG8*) and one downregulated gene (*CAR1*), was remarkably changed in the dual-species biofilm and clinical root caries plaques (Fig. 3; Fig. S3). KEGG analysis also indicated that the alanine, aspartate, and glutamate metabolism pathway, and pantothenate and CoA biosynthesis pathway were upregulated

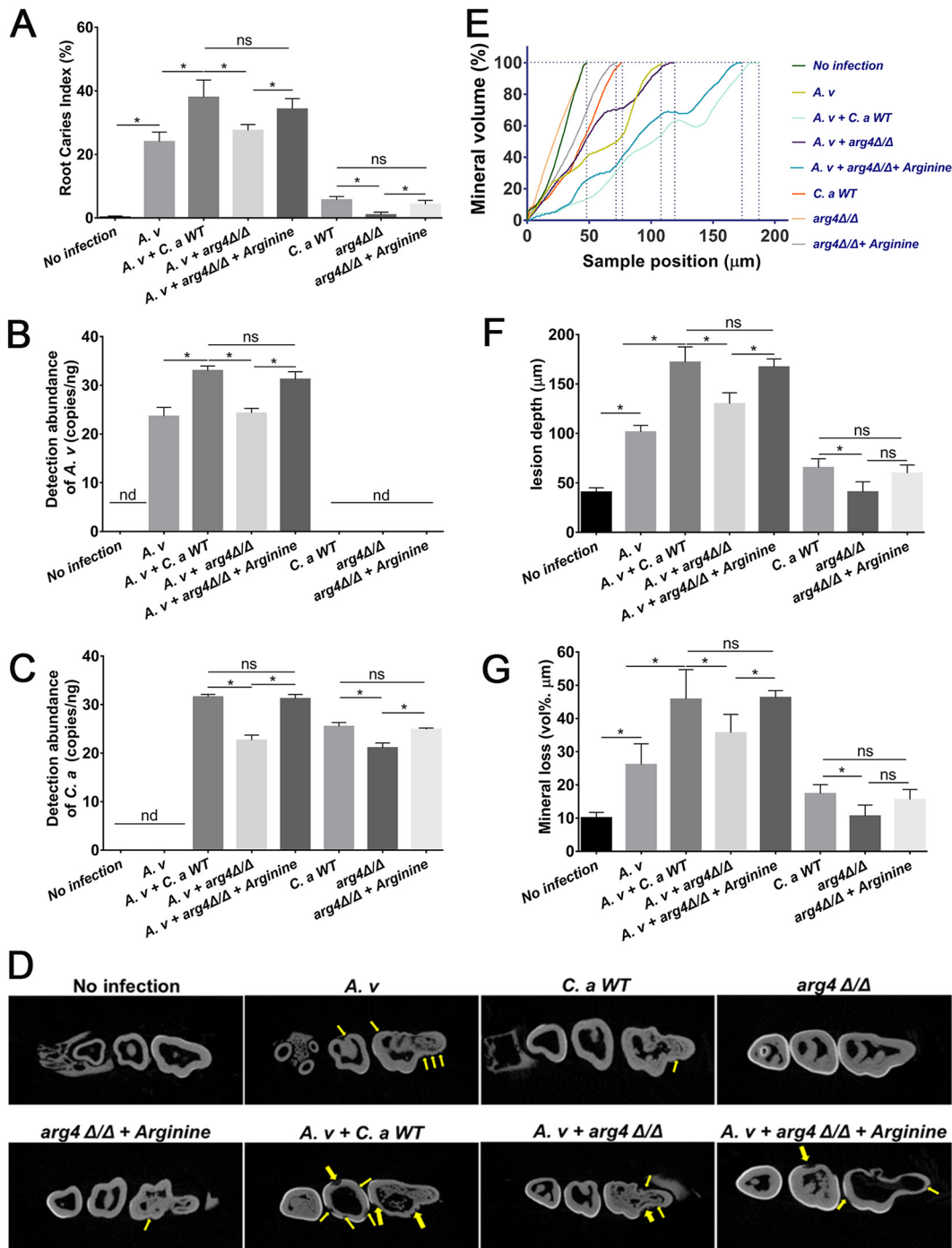


**FIG 6** *C. albicans* arginine biosynthesis pathway regulated the development of root caries and affected the demineralization of the teeth in root caries. (A) Root caries index scores according to Doff's system (\*,  $P < 0.05$ ; ns, not significant). (B, C) Levels of *C. albicans* (B) and *A. viscosus* (C) from the root-caries rats quantified via qPCR (\*,  $P < 0.05$ ; ns, not significant; nd, not detectable). (D) Representative micro-CT images of jaws from uninfected rats and rats infected with *A. viscosus*, *A. viscosus* + *C. albicans*, *A. viscosus*+ *arg4* Δ/Δ, *A. viscosus*+ *arg4* Δ/Δ + Arginine, *C. albicans*, *arg4* Δ/Δ, or *arg4* Δ/Δ + Arginine, respectively. Yellow arrows indicated root carious lesions. (E to G) The mineral volume curves (E), lesion depths (F), and mineral losses (G) of teeth from uninfected rats and rats infected with *A. viscosus*, *A. viscosus* + *C. albicans*, *A. viscosus*+ *arg4* Δ/Δ, or *arg4* Δ/Δ + Arginine, *C. albicans*/*arg4* Δ/Δ, or *arg4* Δ/Δ + Arginine, respectively (\*,  $P < 0.05$ ; ns, not significant).

in the dual-species group (Fig. 3). Glutamate is the essential substrate of arginine biosynthesis, while Acetyl-CoA is one of the important enzymes that metabolize glutamate to produce CoA. The produced glutamate and COA then activate the arginine biosynthesis procedure (35). KEGG analysis also showed that the lysine biosynthesis pathway was significantly

enriched, and the expression levels of genes related to lysine biosynthesis (such as *HOM1*, *LYR22*, *LYR4*, etc.) were significantly upregulated in the dual-species biofilm, while an increase in intracellular lysine can promote arginine secretion (36). These upregulation pathways in the dual-species biofilms indicated that *A. viscosus* might enhance glutamate metabolism and CoA biosynthesis of *C. albicans* and then effectively promote arginine biosynthesis. In addition, *A. viscosus* might also increase the secretion of synthesized arginine through the upregulation of lysine biosynthesis of *C. albicans*. The mechanism of amino acid biosynthesis and metabolism in regulating the interaction between different species is complex. The cross talk between the different amino acid biosynthesis and metabolism from *C. albicans* and *A. viscosus* interactions require further evaluation.

In this study, we evaluated the important role of the arginine biosynthesis pathway of *C. albicans* in its cross-kingdom interaction with *A. viscosus*. The arginine biosynthesis process in the mitochondria and cytoplasm was summarized in Fig. S4A (35, 37). The deletion of *ARG4*, the key gene from the arginine biosynthesis pathway, eliminated synergistic interactions with *A. viscosus*, while the addition of arginine complemented the virulence deficiencies of the *arg4Δ/Δ* mutant in both the single- and dual-species groups (Fig. 5). The addition of arginine could also promote the biofilm formation of *C. albicans*, *A. viscosus*, dual-species, and hyphal formation of *C. albicans* (Fig. 4 and 5), while the neutral amino acids tyrosine and the acidic amino acid glutamate could not promote the biofilm formation of *C. albicans* and *A. viscosus* (unpublished data), indicating the critical role of the arginine biosynthesis pathway of *C. albicans* in its cross-kingdom interaction with *A. viscosus* (Fig. S4B), and targeting this pathway is a practical strategy to reduce the development of root caries. Further investigations are still needed to reveal the mechanisms by which the arginine biosynthesis pathway regulates the growth and virulence of *A. viscosus*.

Arginine is one of the most versatile amino acids in eukaryotic cells and contributes to protein synthesis, cell growth, sexual reproduction, hormone metabolism, signal transduction, osmotic pressure homeostasis, metabolic energy production, nitrogen metabolism, and urea biosynthesis (38, 39). Arginine at the appropriate concentration was essential for the growth and pathogenicity of various microorganisms. Novick et al. (40) isolated an arginine auxotroph *Escherichia coli* mutant and found that it grew slowly in the absence of arginine but grew at a normal rate in the presence of arginine. Hartmann et al. (41) found that arginine could help *Halobacteria* grow in the anaerobic state. Tonon et al. observed that arginine increased the growth of wine lactic acid bacteria (42). Senouci-Rezkallah et al. suggested that arginine stimulated the growth of *Bacillus cereus* under low-acid conditions (43). Vrancken et al. found that arginine enhanced the resistance of *Lactobacillus fermentum* to environmental stresses, such as acid, temperature, salt stress, and osmotic pressure factors (44). Huang's results showed that arginine stimulated the growth of *Streptococcus thermophilus* T1C2 by enhancing resistance to a low intracellular pH under high extracellular osmotic pressure (45). Zhang et al. (38) indicated that three *ARG* genes involved in arginine biosynthesis were essential for growth, conidiogenesis, sexual reproduction, hyphal growth, and pathogenicity in *Magnaporthe oryzae*. The *M. oryzae argΔ/Δ* mutants exhibited significantly delayed conidial germination and decreased pathogenicity, while exogenous arginine could partially restore the infection defects in invasive hyphal growth and pathogenicity (38). Similarly, the addition of arginine could restore the pathogenicity of *Fusarium oxysporum* f. sp. *melonis* arginine auxotroph mutants (46). Our results suggested that the *C. albicans* arginine biosynthesis pathway was significantly activated in the dual-species interactions, while hyphal and biofilm formation were also increased with the significant upregulation of hyphae-associated genes under anaerobic conditions, including *RAS1*, *NCE103*, *GPR1*, *PDE2*, *TPK1*, *UME6*, *MEP2*, *NTH1*, *TOP1*, *PTP3*, etc. (unpublished data). Arginine biosynthesis was reported to be associated with oxidative stress (47), while the transition of *C. albicans* yeast to hyphae also generated ROS as a by-product of oxidative phosphorylation in mitochondria (47, 48). *C. albicans* can also eliminate oxidative stress through the antioxidant pathway and enzymes (49–51). Our

transcriptome analysis indicated that a series of antioxidant genes were significantly upregulated in the dual-species group, including *HSP78*, *HSP21*, *CIP1*, *SOD2*, *SOD5*, *FRE9*, *FRE10*, *CFL1*, *CFL2*, *CFL4*, *CFL11*, *CTR2*, *ZRT1*, and *ZRT2*, etc., indicating the increased capacity of *C. albicans* to eliminate oxidative stress. In addition, the low concentration of additional arginine can directly enhance the growth, biofilm formation, and cariogenic capability of *A. viscosus*, indicating that the upregulated arginine was the key factor in promoting the cross-kingdom interaction. However, the specific mechanisms by which arginine regulates the effects on *A. viscosus* and hyphal growth of *C. albicans* in dual-species combination still need further investigation.

Currently, the relevance of arginine in the oral cavity is still unclear. Arginine could be catabolized by local arginase secreted from host or bacterial cells, such as macrophages and *Porphyromonas gingivalis*, to produce urea and ornithine, thus, increasing the production of polyamines and promote the growth of some bacteria to aggravate the inflammation and tissue destruction (52). Many studies have shown that the arginase activity was positively related to the degree of periodontal inflammation (53–55), indicating the importance of arginine in the development of oral diseases. It is worth noting that arginine could also be an effective therapeutic agent against caries, especially when combined with high-concentration fluoride (56–61), by inhibiting the growth of some cariogenic bacteria, such as *Streptococcus mutans* and *Streptococcus sobrinus* (57), and promoting the remineralization of enamel (60). However, the arginine concentrations used in these studies were high (1.5% mass fraction, or even higher at 8% to 10% mass fraction) (56–61). In our study, arginine was added at a concentration of 0.2%, which was much lower than the potential anti-caries concentrations. The concentration from our study was similar to those that promoted the growth of different microorganisms. Zhang et al. (38) indicated that exogenous arginine supplementation could partially recover the aerial hyphal growth and pathogenicity of *M. oryzae arg Δ/Δ* mutants, but the recovery effect was dependent on the concentration of arginine: the concentration with better recovery effect was 2.5 mM (approximately 0.05% mass fraction), while higher concentration led to the decreased recovery effect. Huang et al. (45) also found that 1.2g/L (approximately 0.12% mass fraction) arginine exhibited the best promotion effect on *S. thermophilus T1C2* growth and that growth was inhibited when the initial arginine concentration exceeded 1.2g/L (approximately 0.12% mass fraction). Similar results were observed by Mira et al. in *Oenococcus oeni* (62). Arginine inhibited *S. mutans* and *S. sobrinus* growth only when the concentration was over 0.4%, while arginine at a concentration  $\leq 0.4\%$  did not affect the growth of *S. mutans* or *S. sobrinus* (57). Our results indicated that arginine at low concentration could enhance the pathogenicity of *A. viscosus* and *C. albicans*, and in the root caries caused by *C. albicans* and *A. viscosus* coinfection. Therefore, the recommendation of arginine-containing caries prevention products and the arginine concentration are worth further careful consideration.

In summary, we identified for the first time that the arginine biosynthesis pathway of *C. albicans* was critical for the regulation of its cross-kingdom interactions with *A. viscosus* and for promoting the occurrence and development of root caries, while targeting this pathway can be a new practical strategy to reduce root caries.

## MATERIALS AND METHODS

**Strains and culture conditions.** *A. viscosus* ATCC 19246 and *C. albicans* WT (SC 5314, ATCC MYA-2876) were obtained from the State Key Laboratory of Oral Diseases. The *ARG4* null mutant of *C. albicans* was also employed to confirm the role of the arginine biosynthesis pathway (Table S1). Briefly, *C. albicans* BWP17 was knocked out in three genes, including *ARG4/URA3/HIS1*. Therefore, as a compromise for the deletion of *URA3* and *HIS1* genes in BWP17 and to obtain the null mutant of *ARG4* (*C. albicans arg4Δ/Δ*), BWP17 was cultured in media with additional uracil and histidine as described previously (63). *A. viscosus* was grown on BHY medium (brain heart infusion medium containing 5 g/l yeast extract) anaerobically (85% N<sub>2</sub>, 10% H<sub>2</sub>, and 5% CO<sub>2</sub>) at 37°C (30) and *C. albicans* WT was grown on yeast extract peptone dextrose (YPD) medium aerobically at 37°C. The coculture mixture (OD<sub>600nm</sub> of each microorganism = 0.1) was grown on yeast nitrogen base (YNB) supplemented with Na<sub>2</sub>HPO<sub>4</sub>·NaH<sub>2</sub>PO<sub>4</sub>, N-acetylglucosamine, casamino acids, and sucrose medium anaerobically (85% N<sub>2</sub>, 10% H<sub>2</sub>, and 5% CO<sub>2</sub>) at 37°C (30). The medium of *C. albicans arg4Δ/Δ* (BWP 17) was supplemented with 0.2% histidine and 0.2% uracil.

**Microbial detection in clinical samples.** In total, 76 volunteers were recruited in our study. Thirty-nine subjects (aged 45 to 75 years old) were clinically diagnosed with root caries by radiography and clinical probing and were divided into RC group, while the other 37 caries-free subjects (aged 45 to 75 years old) acted as the HC group. All participants were in good general health. Ethical approval for the study was granted by the Institutional Review Board of the West China Hospital of Stomatology, Sichuan University (WCHSIRB-D-2020-072). Written informed consent was obtained from each participant that was recruited in this research. The sampling standards were designed as described previously (12). Briefly, in the RC group, after drying and isolating the tooth with sterile cotton rolls, the decayed plaque of root caries was collected with a dental spoon excavator. In the HC group, after drying and isolating the chosen sampling tooth, the supragingival plaque on the root surface was collected with a dental spoon excavator. Each sample was suspended in 1 mL TE buffer and stored at  $-80^{\circ}\text{C}$ .

Total DNA of each sample was extracted with the DNeasy PowerSoil Kit (Qiagen, Valencia, CA, USA). Concentration and quality (A260 nm and A280 nm) measurements of the extracted DNA were performed with a NanoDrop ND-1000 spectrophotometer (Thermo Fisher Scientific, Waltham, MA, USA).

The detection rates of *C. albicans* and *A. viscosus* were determined by PCR (12). The detection abundances of *C. albicans* and *A. viscosus* were quantified by qPCR (12, 64) according to the standard curves of *A. viscosus* and *C. albicans* (65). Correlation analysis and linear regression models were constructed to observe the change trends of the abundances of the two microorganisms. The primers used in this part were listed in Tables S2 and S3.

**Adherence assay.** The adhesion assay was performed as described previously (66). Biofilms were formed in 48-well plates (single species groups: 500  $\mu\text{L}$  *C. albicans*, *arg4 $\Delta$ / $\Delta$*  or *A. viscosus*, respectively, for each well; dual species groups: 250  $\mu\text{L}$  *C. albicans* or *arg4 $\Delta$ / $\Delta$*  + 250  $\mu\text{L}$  *A. viscosus* for each well) under stationary conditions after 24-h incubation in YNBB medium anaerobically (85%  $\text{N}_2$ , 10%  $\text{H}_2$ , and 5%  $\text{CO}_2$ ) at  $37^{\circ}\text{C}$ . The total cells including the cells from the suspension and the cells that were adhered to the well bottom were thoroughly mixed, and then  $\text{OD}_{600\text{nm}}$  was recorded to quantify the total bacteria ( $\text{OD}_{600\text{nm}}$  of total cells). Adherent cells were obtained by removing the suspension and resuspending the remaining cells in equal volume of medium ( $\text{OD}_{600\text{nm}}$  of adherent cells). The adhesion rate was calculated with the formula: adhesion rate =  $\text{OD}_{600\text{nm}}$  of adherent cells/ $\text{OD}_{600\text{nm}}$  of total cells (including the adherent cells and the suspension cells)  $\times 100\%$ .

**Crystal violet assay and CFU counts.** In 96-well plates, 24-h biofilms were produced (single species groups: 200  $\mu\text{L}$  *C. albicans*, *arg4 $\Delta$ / $\Delta$*  or 200  $\mu\text{L}$  *A. viscosus*, respectively, for each well; dual species groups: 100  $\mu\text{L}$  *C. albicans/arg4 $\Delta$ / $\Delta$*  + 100  $\mu\text{L}$  *A. viscosus* for each well) under stationary conditions in YNBB medium anaerobically (85%  $\text{N}_2$ , 10%  $\text{H}_2$ , and 5%  $\text{CO}_2$ ) at  $37^{\circ}\text{C}$ . The total biomass of each biofilm was quantified by crystal violet assay as previously described (30). The biofilms were sequentially fixed with methanol and stained with 0.1% (wt/vol) crystal violet for 15 to 30 min. The suspension was removed, and the cells were resuspended with 33% (vol/vol) glacial acetic acid. Total biomass was determined with  $\text{OD}_{600\text{nm}}$  of the suspension. To quantify the viable cells in biofilms, CFU counts were performed as described previously (30). Briefly, the biofilms were scraped off and resuspended with equal volume of medium. Then, the suspensions were 1:10 serially diluted and viable biofilm cells were quantified by CFU counts after plating the proper dilutions on YPD agar and incubating for 24 h.

**Scanning electron microscopy observation and fluorescence *in situ* hybridization observation.** To observe the biofilm structure, scanning electron microscopy (SEM) observation and fluorescence *in situ* hybridization (FISH) observations were performed. Then, 24-h biofilm samples were produced on sterile glass slides at the bottom of each well of 24-well plates (single species groups: 1,000  $\mu\text{L}$  *C. albicans*, *arg4 $\Delta$ / $\Delta$*  or *A. viscosus*, respectively, for each well; dual species groups: 500  $\mu\text{L}$  *C. albicans/arg4 $\Delta$ / $\Delta$*  + 500  $\mu\text{L}$  *A. viscosus* for each well) under stationary conditions in YNBB medium anaerobically (85%  $\text{N}_2$ , 10%  $\text{H}_2$ , and 5%  $\text{CO}_2$ ) at  $37^{\circ}\text{C}$ . SEM analysis was carried out as previously described (30). Each sample was observed by SEM imaging (FEI, Hillsboro, USA) at  $5,000\times$  magnification. The FISH procedure was performed as previously described (30) and observed with an Eclipse FV1000 inverted confocal laser scanning microscope (Olympus Corporation, Japan). The sequences of oligonucleotide probes (30) were listed in Table S4. The probes were synthesized by Sangon Biotech (Shanghai, China).

**Anthrone-sulfuric acid assay.** The water-insoluble EPS production ability of 24-h biofilms were analyzed by anthrone-sulfuric acid assay. In 96-well plates, 24-h biofilms were produced (single species groups: 200  $\mu\text{L}$  *C. albicans*, *arg4 $\Delta$ / $\Delta$*  or *A. viscosus*, respectively, for each well; dual species groups: 100  $\mu\text{L}$  *C. albicans/arg4 $\Delta$ / $\Delta$*  + 100  $\mu\text{L}$  *A. viscosus* for each well) under stationary conditions in YNBB medium anaerobically (85%  $\text{N}_2$ , 10%  $\text{H}_2$ , and 5%  $\text{CO}_2$ ) at  $37^{\circ}\text{C}$ . The biofilms were resuspended, and the precipitates were obtained and washed with sterile water to remove the water-soluble EPS. Then, each water-insoluble EPS sample was extracted with 0.4M NaOH under agitation for 2 h. Three milliliters of 0.2% anthrone-sulfuric acid reagent was mixed into each supernatant sample and then incubated in a water bath at  $95^{\circ}\text{C}$  for 6 min. The water-soluble EPS production ability was determined by  $\text{OD}_{625\text{nm}}$ .

**RNA sequencing and data analysis.** Total RNA in each sample was extracted with TRIzol reagent (Invitrogen, Carlsbad, USA). RNA sequencing (RNA-Seq) was performed by Illumina NovaSeq (Shanghai Personal Biotechnology Co., Ltd., China) as described elsewhere (67).

A total of 6,030 genes were analyzed. Differential gene expression analysis was performed using fragments per kilobase per million (FPKM) values. The Pearson correlation coefficient was estimated to analyze the correlation of gene expression levels between samples and principal-component analysis (PCA) was used to cluster samples in each group. Differentially expressed genes (DEGs) were defined with the criteria of absolute  $\log_2$ -fold change (FC)  $> 1$  and adjusted  $P$  value  $< 0.05$ . DEGs were regarded as upregulated if their expression levels in dual-species biofilm samples were higher than those in the *Candida albicans* single-species biofilm, and vice versa. The expression of DEGs in each treatment was

visualized as a volcano plot and heatmap. DEGs were submitted for functional enrichment analyses to Gene Orthology (GO) and KEGG annotations.

**Analysis of the gene expression levels in biofilms.** The biofilms were collected and quantitative PCR (qPCR) was performed to evaluate the expression levels of arginine biosynthesis-associated DEGs (*ARG1*, *ARG3*, *ARG4*, etc.). RNA isolation with TRIzol Reagent (Invitrogen, Carlsbad, CA, USA) and purification procedures were conducted as previously described (68). To synthesize first-strand cDNAs, RNA reverse transcription was performed with a PrimeScript RT reagent kit with gDNA Eraser (TaKaRa Biotechnology, Japan). Specific primers for the tested genes were designed using Primer3Plus (<http://www.primer3plus.com/cgi-bin/dev/primer3plus.cgi>) and were listed in Table S5. The qPCR mixture and procedure were carried out as previously described (68). Relative fold changes in the expression of associated genes were evaluated with the  $2^{-\Delta\Delta Ct}$  method (69), and the 18S rRNA gene expression level was used to normalize the expression level of different genes.

**Gene expression analysis in clinical samples.** In total, another 20 volunteers were recruited. Ten subjects (aged 45 to 75 years) were clinically diagnosed with root caries by radiography and clinical probing and were divided into the RC group, while the other 10 caries-free subjects (aged 45 to 75 years) acted as the HC group. All participants were in good general health. Ethical approval for the study was granted by the Institutional Review Board of the West China Hospital of Stomatology, Sichuan University (WCHSIRB-D-2020-072). Clinical plaque samples were collected as described above. RNA from each sample was extracted with TRIzol Reagent (Invitrogen, Carlsbad, CA, USA) and qPCR was performed to compare the expression levels of genes in the arginine biosynthesis pathway in the RC group and HC group.

**Root caries rat model.** The rat model was established to investigate the promotion ability of *C. albicans* and *A. viscosus* interactions on root caries and the corresponding pathogenesis *in vivo*. The experiment was started after approval was obtained from the animal research committee of West China School of Stomatology, Sichuan University (WCHSIRB-D-2020-127). Male 17-day-old specific pathogen free (SPF) Sprague-Dawley (SD) rats purchased from Dashuo Inc. (Chengdu, China) were used for the *in vivo* experiment (five rats in each group). The root caries model was established as described in a previous study (12). Briefly, the rats were fed with 5% (wt/vol) sucrose-containing water and caries-promoting diet (Diet 2000) every day. The rats were infected daily for 3 consecutive days with *A. viscosus*, *C. albicans* WT, *arg4* $\Delta/\Delta$  mutant, and *C. albicans*-*A. viscosus* combinations according to the designated groups ( $10^9$  CFU/mL, 200  $\mu$ L each rat). Ten days after the initial infection, the rats were anesthetized and underwent the gingivectomy surgery. On days 38 to 40, the rats were reinoculated with microbes. On day 66, the rats were sacrificed and the jaws were removed aseptically. The dental plaque of each jaw was collected to detect the abundances of microorganisms through qPCR as described above. Each jaw was stained with mercurochrome for 18 h to record the root caries score according to Doff's criterion (70). Then, the jaws were subjected to the micro-computed tomography ( $\mu$ CT 50, SCANCO Medical AG, Brüttisellen, Switzerland) analysis (71). They were scanned at a medium resolution, with parameters of 70 kVp and 200  $\mu$ A. Each sample was rotated 360° within 14.3 min. SCANCO evaluation software version 1.1.11.0 (SCANCO Medical AG) was used to acquire and analyze Micro-CT images. A line in the selected sectional view of each jaw was chosen as the region of interest (ROI) to be quantitatively analyzed. The mineral volume, lesion depth, and mineral loss of the ROI were measured by SCANCO evaluation software to evaluate the degree of root caries.

**Statistical analysis.** For the clinical sample detections, differences between the two groups were compared with *t* test or Kruskal-Wallis analysis after a homogeneity test of variance with Levene's test. For the other experiments, differences among multiple groups were compared using one-way ANOVA and *post hoc* Tukey's multiple comparisons after a homogeneity test of variance with Levene's test, and two independent groups were analyzed with *t* test after the homogeneity of variance test. Statistical analysis was performed using SPSS software (Version 20.0; IBM Corp., Armonk, USA) with a significance level of 0.05, and then all figures were generated with GraphPad Prism7 software (version 7.00 for Windows; GraphPad Prism, Inc, La Jolla, USA).

**Data availability.** RNA sequencing data have been deposited in the public database Sequence Read Archive with accession no. (PRJNA753272). All data sets generated and/or analyzed in the current study are available from the corresponding author on reasonable request.

## SUPPLEMENTAL MATERIAL

Supplemental material is available online only.

**SUPPLEMENTAL FILE 1**, PDF file, 0.4 MB.

## ACKNOWLEDGMENTS

This work was supported by the National Natural Science Foundation of China (82071111, 81870778, 81600858, 81991500, 81991501), Key Research and Development Projects of Science and Technology Department of Sichuan Province (2020YFSY0019, 2021YFQ0064), and Applied Basic Research Programs of Sichuan Province (2020YJ0227).

We declare no conflicts of interest.

## REFERENCES

1. Anonymous. 2018. Global, regional, and national incidence, prevalence, and years lived with disability for 354 diseases and injuries for 195 countries and territories, 1990-2017: a systematic analysis for the Global Burden of Disease Study 2017. *Lancet* 392:1789-1858. [https://doi.org/10.1016/S0140-6736\(18\)32279-7](https://doi.org/10.1016/S0140-6736(18)32279-7).
2. Cai J, Palamara J, Manton DJ, Burrow MF. 2018. Status and progress of treatment methods for root caries in the last decade: a literature review. *Aust Dent J* 63:34-54. <https://doi.org/10.1111/adj.12550>.
3. Hayes M, Burke F, Allen PF. 2017. Incidence, prevalence and global distribution of root caries. *Monogr Oral Sci* 26:1-8. <https://doi.org/10.1159/000479301>.

4. Gao YB, Hu T, Zhou XD, Shao R, Cheng R, Wang GS, Yang YM, Li X, Yuan B, Xu T, Wang X, Feng XP, Tai BJ, Hu Y, Lin HC, Wang B, Si Y, Wang CX, Zheng SG, Liu XN, Rong WS, Wang WJ, Yin W. 2018. How root caries differs between middle-aged people and the elderly: findings from the 4th National Oral Health Survey of China. *Chin J Dent Res* 21:221–229. <https://doi.org/10.3290/j.cjdr.a41078>.
5. WHO Center for Health Development. 2006. 8020 better oral health for older people. World Health Organization, Geneva, Switzerland.
6. Syed SA, Loesche WJ, Pape HL, Jr, Grenier E. 1975. Predominant cultivable flora isolated from human root surface caries plaque. *Infect Immun* 11:727–731. <https://doi.org/10.1128/iai.11.4.727-731.1975>.
7. Ellen RP, Banting DW, Fillery ED. 1985. Longitudinal microbiological investigation of a hospitalized population of older adults with a high root surface caries risk. *J Dent Res* 64:1377–1381. <https://doi.org/10.1177/00220345850640121001>.
8. Liu T, Gibbons RJ, Hay DI, Skobe Z. 1991. Binding of Actinomyces viscosus to collagen: association with the type 1 fibrillar adhesin. *Oral Microbiol Immunol* 6:1–5. <https://doi.org/10.1111/j.1399-302x.1991.tb00443.x>.
9. Komiyama K, Khandelwal RL, Heinrich SE. 1988. Glycogen synthetic and degradative activities by Actinomyces viscosus and Actinomyces naeslundii of root surface caries and noncaries sites. *Caries Res* 22:217–225. <https://doi.org/10.1159/000261109>.
10. Zhou Y, Cheng L, Liao B, Shi Y, Niu Y, Zhu C, Ye X, Zhou X, Ren B. 2021. Candida albicans CHK1 gene from two-component system is essential for its pathogenicity in oral candidiasis. *Appl Microbiol Biotechnol* 105:2485–2496. <https://doi.org/10.1007/s00253-021-11187-0>.
11. Bachtiar EW, Bachtiar BM. 2018. Relationship between Candida albicans and Streptococcus mutans in early childhood caries, evaluated by quantitative PCR. *F1000Res* 7:1645. <https://doi.org/10.12688/f1000research.16275.2>.
12. Du Q, Ren B, He J, Peng X, Guo Q, Zheng L, Li J, Dai H, Chen V, Zhang L, Zhou X, Xu X. 2021. Candida albicans promotes tooth decay by inducing oral microbial dysbiosis. *ISME J* 15:894–908. <https://doi.org/10.1038/s41396-020-00823-8>.
13. Beighton D, Ludford R, Clark DT, Brailsford SR, Pankhurst CL, Tinsley GF, Fiske J, Lewis D, Daly B, Khalifa N. 1995. Use of CHROMagar Candida medium for isolation of yeasts from dental samples. *J Clin Microbiol* 33:3025–3027. <https://doi.org/10.1128/jcm.33.11.3025-3027.1995>.
14. Mayer FL, Wilson D, Hube B. 2013. Candida albicans pathogenicity mechanisms. *Virulence* 4:119–128. <https://doi.org/10.4161/viru.22913>.
15. Pereira D, Seneviratne CJ, Koga-Ito CY, Samaranyake LP. 2018. Is the oral fungal pathogen Candida albicans a cariogen? *Oral Dis* 24:518–526. <https://doi.org/10.1111/odi.12691>.
16. Lobo CIV, Rinaldi TB, Christiano CMS, De Sales Leite L, Barbugli PA, Klein MI. 2019. Dual-species biofilms of Streptococcus mutans and Candida albicans exhibit more biomass and are mutually beneficial compared with single-species biofilms. *J Oral Microbiol* 11:1581520. <https://doi.org/10.1080/20002297.2019.1581520>.
17. Bamford CV, d'Mello A, Nobbs AH, Dutton LC, Vickerman MM, Jenkinson HF. 2009. Streptococcus gordonii modulates Candida albicans biofilm formation through intergeneric communication. *Infect Immun* 77:3696–3704. <https://doi.org/10.1128/IAI.00438-09>.
18. Diaz PI, Xie Z, Sobue T, Thompson A, Biyikoglu B, Ricker A, Ikonomou L, Dongari-Bagtzoglou A. 2012. Synergistic interaction between Candida albicans and commensal oral streptococci in a novel in vitro mucosal model. *Infect Immun* 80:620–632. <https://doi.org/10.1128/IAI.05896-11>.
19. Chen X, Zhou X, Liao B, Zhou Y, Cheng L, Ren B. 2021. The cross-kingdom interaction between Helicobacter pylori and Candida albicans. *PLoS Pathog* 17:e1009515. <https://doi.org/10.1371/journal.ppat.1009515>.
20. Arzmi MH, Dashper S, Catmull D, Cirillo N, Reynolds EC, McCullough M. 2015. Coaggregation of Candida albicans, Actinomyces naeslundii and Streptococcus mutans is Candida albicans strain dependent. *FEMS Yeast Res* 15:fov038. <https://doi.org/10.1093/femsyr/fov038>.
21. Cavalcanti IM, Nobbs AH, Ricomini-Filho AP, Jenkinson HF, Del Bel Cury AA. 2016. Interkingdom cooperation between Candida albicans, Streptococcus oralis and Actinomyces oris modulates early biofilm development on denture material. *Pathog Dis* 74.
22. Souza JGS, Bertolini M, Thompson A, Barão VAR, Dongari-Bagtzoglou A. 2020. Biofilm interactions of Candida albicans and mitis group streptococci in a titanium-mucosal interface model. *Appl Environ Microbiol* 86. <https://doi.org/10.1128/AEM.02950-19>.
23. Sobue T, Diaz P, Xu H, Bertolini M, Dongari-Bagtzoglou A. 2016. Experimental models of C. albicans-streptococcal co-infection. *Methods Mol Biol* 1356:137–152. [https://doi.org/10.1007/978-1-4939-3052-4\\_10](https://doi.org/10.1007/978-1-4939-3052-4_10).
24. Cavalcanti YW, Wilson M, Lewis M, Del-Bel-Cury AA, da Silva WJ, Williams DW. 2016. Modulation of Candida albicans virulence by bacterial biofilms on titanium surfaces. *Biofouling* 32:123–134. <https://doi.org/10.1080/08927014.2015.1125472>.
25. Falsetta ML, Klein MI, Colonne PM, Scott-Anne K, Gregoire S, Pai CH, Gonzalez-Begne M, Watson G, Krysan DJ, Bowen WH, Koo H. 2014. Symbiotic relationship between Streptococcus mutans and Candida albicans synergizes virulence of plaque biofilms in vivo. *Infect Immun* 82:1968–1981. <https://doi.org/10.1128/IAI.00087-14>.
26. Kim D, Sengupta A, Niepa TH, Lee BH, Weljie A, Freitas-Blanco VS, Murata RM, Stebe KJ, Lee D, Koo H. 2017. Candida albicans stimulates Streptococcus mutans microcolony development via cross-kingdom biofilm-derived metabolites. *Sci Rep* 7:41332. <https://doi.org/10.1038/srep41332>.
27. Fehrmann C, Jurk K, Bertling A, Seidel G, Fegeler W, Kehrel BE, Peters G, Becker K, Heilmann C. 2013. Role for the fibrinogen-binding proteins coagulase and Efb in the Staphylococcus aureus-Candida interaction. *Int J Med Microbiol* 303:230–238. <https://doi.org/10.1016/j.ijmm.2013.02.011>.
28. Hu Y, Niu Y, Ye X, Zhu C, Tong T, Zhou Y, Zhou X, Cheng L, Ren B. 2021. Staphylococcus aureus synergized with Candida albicans to increase the pathogenesis and drug resistance in cutaneous abscess and peritonitis murine models. *Pathogens* 10:1036. <https://doi.org/10.3390/pathogens10081036>.
29. Deng L, Zou L, Wu J, Liu H, Luo T, Zhou X, Li W, Ren B. 2019. Voriconazole inhibits cross-kingdom interactions between Candida albicans and Actinomyces viscosus through the ergosterol pathway. *Int J Antimicrob Agents* 53:805–813. <https://doi.org/10.1016/j.ijantimicag.2019.02.010>.
30. Deng L, Li W, He Y, Wu J, Ren B, Zou L. 2019. Cross-kingdom interaction of Candida albicans and Actinomyces viscosus elevated cariogenic virulence. *Arch Oral Biol* 100:106–112. <https://doi.org/10.1016/j.archoralbio.2019.02.008>.
31. Wierichs RJ, Meyer-Lueckel H. 2015. Systematic review on noninvasive treatment of root caries lesions. *J Dent Res* 94:261–271. <https://doi.org/10.1177/0022034514557330>.
32. Janus MM, Willems HM, Krom BP. 2016. Candida albicans in multispecies oral communities; a keystone commensal? *Adv Exp Med Biol* 931:13–20. [https://doi.org/10.1007/5584\\_2016\\_5](https://doi.org/10.1007/5584_2016_5).
33. Sosroseno W, Herminajeng E, Bird P. 2015. The effect of immune status, age and genetic background on induction of oral tolerance to Actinomyces viscosus in mice. *Biomed Pharmacother* 70:294–298. <https://doi.org/10.1016/j.biopha.2014.12.039>.
34. Morse DJ, Wilson MJ, Wei X, Bradshaw DJ, Lewis MAO, Williams DW. 2019. Modulation of Candida albicans virulence in in vitro biofilms by oral bacteria. *Lett Appl Microbiol* 68:337–343. <https://doi.org/10.1111/lam.13145>.
35. Turner SA, Ma Q, Ola M, Martinez de San Vicente K, Butler G. 2018. Dal81 regulates expression of arginine metabolism genes in Candida parapsilosis. *mSphere* 3. <https://doi.org/10.1128/mSphere.00028-18>.
36. Marbaniang CN, Gowrishankar J. 2012. Transcriptional cross-regulation between Gram-negative and Gram-positive bacteria, demonstrated using ArgP-argO of Escherichia coli and LysG-lysE of Corynebacterium glutamicum. *J Bacteriol* 194:5657–5666. <https://doi.org/10.1128/JB.00947-12>.
37. Gibbons GF, Howard DH. 1986. Arginine auxotrophs of Candida albicans deficient in argininosuccinate lyase. *J Gen Microbiol* 132:263–268. <https://doi.org/10.1099/00221287-132-2-263>.
38. Zhang Y, Shi H, Liang S, Ning G, Xu N, Lu J, Liu X, Lin F. 2015. MoARG1, MoARG5,6 and MoARG7 involved in arginine biosynthesis are essential for growth, conidiogenesis, sexual reproduction, and pathogenicity in Magnaporthe oryzae. *Microbiol Res* 180:11–22. <https://doi.org/10.1016/j.micres.2015.07.002>.
39. Wu G, Bazer FW, Davis TA, Kim SW, Li P, Marc Rhoads J, Carey Satterfield M, Smith SB, Spencer TE, Yin Y. 2009. Arginine metabolism and nutrition in growth, health and disease. *Amino Acids* 37:153–168. <https://doi.org/10.1007/s00726-008-0210-y>.
40. Novick RP, Maas WK. 1961. Control by endogenously synthesized arginine of the formation of ornithine transcarbamylase in Escherichia coli. *J Bacteriol* 81:236–240. <https://doi.org/10.1128/jb.81.2.236-240.1961>.
41. Hartmann R, Sickingner HD, Oesterheld D. 1980. Anaerobic growth of halo-bacteria. *Proc Natl Acad Sci U S A* 77:3821–3825. <https://doi.org/10.1073/pnas.77.7.3821>.
42. Tonon T, Lonvaud-Funel A. 2000. Metabolism of arginine and its positive effect on growth and revival of Oenococcus oeni. *J Appl Microbiol* 89:526–531. <https://doi.org/10.1046/j.1365-2672.2000.01142.x>.
43. Senouci-Rezkallah K, Schmitt P, Jobin MP. 2011. Amino acids improve acid tolerance and internal pH maintenance in Bacillus cereus ATCC14579 strain. *Food Microbiol* 28:364–372. <https://doi.org/10.1016/j.fm.2010.09.003>.
44. Vrancken G, Rimaux T, Wouters D, Leroy F, De Vuyst L. 2009. The arginine deiminase pathway of Lactobacillus fermentum IMDO 130101 responds

- to growth under stress conditions of both temperature and salt. *Food Microbiol* 26:720–727. <https://doi.org/10.1016/j.fm.2009.07.006>.
45. Huang S, Ai ZW, Sun XM, Liu GF, Zhai S, Zhang M, Chen H, Feng Z. 2016. Influence of arginine on the growth, arginine metabolism and amino acid consumption profiles of *Streptococcus thermophilus* T1C2 in controlled pH batch fermentations. *J Appl Microbiol* 121:746–756. <https://doi.org/10.1111/jam.13221>.
  46. Namiki F, Matsunaga M, Okuda M, Inoue I, Nishi K, Fujita Y, Tsuge T. 2001. Mutation of an arginine biosynthesis gene causes reduced pathogenicity in *Fusarium oxysporum* f. sp. melonis. *Mol Plant Microbe Interact* 14: 580–584. <https://doi.org/10.1094/MPMI.2001.14.4.580>.
  47. Dutton LC, Paszkiewicz KH, Silverman RJ, Splatt PR, Shaw S, Nobbs AH, Lamont RJ, Jenkinson HF, Ramsdale M. 2016. Transcriptional landscape of trans-kingdom communication between *Candida albicans* and *Streptococcus gordonii*. *Mol Oral Microbiol* 31:136–161. <https://doi.org/10.1111/omi.12111>.
  48. Schröter C, Hipler UC, Wilmer A, Künkel W, Wollina U. 2000. Generation of reactive oxygen species by *Candida albicans* in relation to morphogenesis. *Arch Dermatol Res* 292:260–264. <https://doi.org/10.1007/s004030050484>.
  49. Mayer FL, Wilson D, Jacobsen ID, Miramón P, Slesiona S, Bohovych IM, Brown AJ, Hube B. 2012. Small but crucial: the novel small heat shock protein Hsp21 mediates stress adaptation and virulence in *Candida albicans*. *PLoS One* 7:e38584. <https://doi.org/10.1371/journal.pone.0038584>.
  50. Dantas AdS, Day A, Ikeh M, Kos I, Achan B, Quinn J. 2015. Oxidative stress responses in the human fungal pathogen, *Candida albicans*. *Biomolecules* 5:142–165. <https://doi.org/10.3390/biom5010142>.
  51. Lorenz MC, Bender JA, Fink GR. 2004. Transcriptional response of *Candida albicans* upon internalization by macrophages. *Eukaryot Cell* 3:1076–1087. <https://doi.org/10.1128/EC.3.5.1076-1087.2004>.
  52. Grandvaux N, Gaboriau F, Harris J, ten Oever BR, Lin R, Hiscott J. 2005. Regulation of arginase II by interferon regulatory factor 3 and the involvement of polyamines in the antiviral response. *FEBS J* 272:3120–3131. <https://doi.org/10.1111/j.1742-4658.2005.04726.x>.
  53. Gheren LW, Cortelli JR, Rodrigues E, Holzhausen M, Saad WA. 2008. Periodontal therapy reduces arginase activity in saliva of patients with chronic periodontitis. *Clin Oral Invest* 12:67–72. <https://doi.org/10.1007/s00784-007-0146-8>.
  54. Sun J, Wang D, Wang A, Wang Q. 2011. Study on the difference of arginase expression between normal and periodontitis gingival tissues (in Chinese). *Contemporary Medicine* 17.
  55. Sun J, Wang A, Gao Y. 2012. Expression of arginase in periodontal tissues of experimental periodontitis in rats (in Chinese). *Chin J Conserv Dent* 22: 445.
  56. Kuriki N, Asahi Y, Sotozono M, Machi H, Noiri Y, Hayashi M, Ebisu S. 2021. Next-generation sequencing for determining the effect of arginine on human dental biofilms using an in situ model. *Pharmacy (Basel)* 9:18. <https://doi.org/10.3390/pharmacy9010018>.
  57. Huang X, Zhang K, Deng M, Exterkate RAM, Liu C, Zhou X, Cheng L, Ten Cate JM. 2017. Effect of arginine on the growth and biofilm formation of oral bacteria. *Arch Oral Biol* 82:256–262. <https://doi.org/10.1016/j.archoralbio.2017.06.026>.
  58. Wolff MS, Schenkel AB. 2018. The anticaries efficacy of a 1.5% arginine and fluoride toothpaste. *Adv Dent Res* 29:93–97. <https://doi.org/10.1177/0022034517735298>.
  59. Nascimento MM, Alvarez AJ, Huang X, Browngardt C, Jenkins R, Sinhoret MC, Ribeiro APD, Dilbone DA, Richards VP, Garrett TJ, Burne RA. 2019. Metabolic profile of supragingival plaque exposed to arginine and fluoride. *J Dent Res* 98:1245–1252. <https://doi.org/10.1177/0022034519869906>.
  60. Bijle MNA, Ekambaram M, Lo EC, Yiu CKY. 2018. The combined enamel remineralization potential of arginine and fluoride toothpaste. *J Dent* 76: 75–82. <https://doi.org/10.1016/j.jdent.2018.06.009>.
  61. Agnello M, Cen L, Tran NC, Shi W, McLean JS, He X. 2017. Arginine improves pH homeostasis via metabolism and microbiome modulation. *J Dent Res* 96:924–930. <https://doi.org/10.1177/0022034517707512>.
  62. Mira De Orduña R, Patchett ML, Liu SQ, Pilon GJ. 2001. Growth and arginine metabolism of the wine lactic acid bacteria *Lactobacillus buchneri* and *Oenococcus oeni* at different pH values and arginine concentrations. *Appl Environ Microbiol* 67:1657–1662. <https://doi.org/10.1128/AEM.67.4.1657-1662.2001>.
  63. Ghosh S, Navarathna DH, Roberts DD, Cooper JT, Atkin AL, Petro TM, Nickerson KW. 2009. Arginine-induced germ tube formation in *Candida albicans* is essential for escape from murine macrophage line RAW 264.7. *Infect Immun* 77:1596–1605. <https://doi.org/10.1128/IAI.01452-08>.
  64. Liu B, Zhang W, Gou S, Huang H, Yao J, Yang Z, Liu H, Zhong C, Liu B, Ni J, Wang R. 2017. Intramolecular cyclization of the antimicrobial peptide Pol-ybia-MPI with triazole stapling: influence on stability and bioactivity. *J Pept Sci* 23:824–832. <https://doi.org/10.1002/psc.3031>.
  65. Lee C, Kim J, Shin SG, Hwang S. 2006. Absolute and relative QPCR quantification of plasmid copy number in *Escherichia coli*. *J Biotechnol* 123: 273–280. <https://doi.org/10.1016/j.jbiotec.2005.11.014>.
  66. Hasan S, Danishuddin M, Khan AU. 2015. Inhibitory effect of zingiber officinale towards *Streptococcus mutans* virulence and caries development: in vitro and in vivo studies. *BMC Microbiol* 15:1. <https://doi.org/10.1186/s12866-014-0320-5>.
  67. Guo J, Ma Z, Peng J, Mo J, Li Q, Guo J, Yang F. 2021. Transcriptomic analysis of *Raphidocelis subcapitata* exposed to erythromycin: the role of DNA replication in hormesis and growth inhibition. *J Hazard Mater* 402: 123512. <https://doi.org/10.1016/j.jhazmat.2020.123512>.
  68. Xu X, Zhou XD, Wu CD. 2011. The tea catechin epigallocatechin gallate suppresses cariogenic virulence factors of *Streptococcus mutans*. *Antimicrob Agents Chemother* 55:1229–1236. <https://doi.org/10.1128/AAC.01016-10>.
  69. Pfaffl MW. 2001. A new mathematical model for relative quantification in real-time RT-PCR. *Nucleic Acids Res* 29:e45. <https://doi.org/10.1093/nar/29.9.e45>.
  70. Doff RS, Rosen S, App G. 1977. Root surface caries in the molar teeth of Rice rats. I. A method for quantitative scoring. *J Dent Res* 56:1013–1016. <https://doi.org/10.1177/00220345770560080301>.
  71. Wu T, Li B, Zhou X, Hu Y, Zhang H, Huang Y, Xu HHK, Guo Q, Li M, Feng M, Peng X, Weir MD, Cheng L, Ren B. 2018. Evaluation of novel anticaries adhesive in a secondary caries animal model. *Caries Res* 52:14–21. <https://doi.org/10.1159/000481832>.